Journal of Cancer Research and Clinical Oncology (2019) 145:1297–1311
https://doi.org/10.1007/s00432-019-02898-z

ORIGINAL ARTICLE – CANCER RESEARCH

TRPM2 mediates distruption of autophagy machinery and correlates with the grade level in prostate cancer

Ahmet Tektemur[1] · Seda Ozaydin[1] · Ebru Etem Onalan[1] · Nalan Kaya[2] · Tuncay Kuloglu[2] · İbrahim Hanifi Ozercan[3] · Suat Tekin[4] · Halit Mohammed Elyas[1]

Received: 2 January 2019 / Accepted: 13 March 2019 / Published online: 19 March 2019

Abstract

Purpose Transient receptor potential melastatin 2 (TRPM2), a calcium-permeable ion channel, is shown as a prognostic marker candidate in prostate cancer (PCa) and an important regulator of autophagy. We aimed to determine the changes in TRPM2 and autophagic–apoptotic gene expression levels in human prostate adenocarcinomas, and to investigate the affect of TRPM2 on autophagic pathways in PC-3 cell line.

Methods Human prostate tissues were classified considering the grade levels and were divided into the control, BPH, and grade 1–5 groups. mRNA expression levels of genes were determined by qPCR. In addition, TRPM2 was evaluated immunohistochemically for each group. In PC-3 cell line, TRPM2 was silenced through siRNA transfection, and autophagy induction was analyzed by acridine orange (AO) staining.

Results The qPCR and immunoreactivity results showed that the increased TRPM2 expression levels in human PCa samples were paralleled with higher grade levels. The autophagic–apoptotic gene expressions showed high variability in different grade levels. Also, silencing TRPM2 in PC-3 cells altered autophagic gene expressions and caused autophagy induction according to the AO staining results.

Conclusion We showed that the autophagy–TRPM2 association may take place in the molecular basis of PCa and accordingly this connection may be targeted as a new therapeutic approach in PCa.

Keywords Prostate cancer · Ion channels · Transient receptor potential melastatin 2 (TRPM2) · Autophagy · Gene expression

Introduction

Prostate cancer (PCa) is the second most common cancer worldwide for males (Ferlay et al. 2015) and is one of the leading causes of cancer-related death (Borley and Feneley 2009). Although it has a high incidence, still little is known about the etiology (Reynolds and Kyprianou 2006). While the majority of localized prostate cancers can be controlled with surgery and/or radiation, metastatic disease remains a lethal disease with no curative options (Palmbos and Hussain 2016). Studies are carried out at the molecular level for the induction of apoptosis (Reynolds and Kyprianou 2006) or for the inhibition of cancer invasion (Bao et al. 2005) to create new treatment options but still more efforts should be made to develop protective strategies that will reduce the negative consequences of PCa (Mahmoud et al. 2014).

Ion channels, regulating the flow of ions across biological membranes (Huang and Yan 2014), may have oncogenic or tumor suppressor properties in different cancer types (Lang and Stournaras 2014). Alterations in the calcium (Ca^{2+}) channels affect the intracellular Ca^{2+} levels and Ca^{2+}-dependent processes such as proliferation, apoptosis (Prevarskaya et al. 2007) and autophagy (Kondratskyi et al. 2013). Recently, ion channels have been defined as major regulators of both basal and induced autophagy

✉ Ahmet Tektemur
atektemur@firat.edu.tr

[1] Department of Medical Biology, Faculty of Medicine, Firat University, Elazig, Turkey

[2] Department of Histology, Faculty of Medicine, Firat University, Elazig, Turkey

[3] Department of Medical Pathology, Faculty of Medicine, Firat University, Elazig, Turkey

[4] Department of Physiology, Faculty of Medicine, Inonu University, Malatya, Turkey

(Kondratskyi et al. 2018). Autophagy is a cellular catabolic process in which various molecules are degraded and recycled to maintain cellular homeostasis (Ravikumar et al. 2010). Autophagy consists of several phases such as induction, nucleation, elongation, fusion, and degradation. In each stage of the autophagy, multiple autophagy-related genes (ATG) play a role (Subramani and Malhotra 2013). It is stated that autophagy deregulation can facilitate tumor development by affecting many physiological processes and in some cases can suppress tumor formation. (Choi et al. 2013; White 2015). Recently, it has been reported that increases and decreases in some autophagic gene expressions in several PCa investigations lead to disruption of autophagic mechanisms (Ouyang et al. 2013; Morell et al. 2016).

Transient receptor potential melastatin 2 (TRPM2) ion channel is a potential candidate to contribute to Ca^{2+} homeostasis in PCa cells (Flourakis and Prevarskaya 2009). Also, increased TRPM2 expression in PCa has been suggested that it can be used as a prognostic marker (Prevarskaya et al. 2007). TRPM2-dependent Ca^{2+} influx induced by oxidative stress inhibits autophagy, leading to cells becoming more sensitive to death. However, oxidative stress stimulates autophagy (and not cell death) in the absence of the TRPM2-dependent Ca^{+2} influx (Wang et al. 2016). TRPM2 inhibition may be beneficial for inducing apoptosis and autophagy and increase the effectiveness of chemotherapy regimens (Zeng et al. 2010).

Although the roles of the TRPM2 ion channel in proliferation and apoptosis are largely determined, the knowledges about the mechanisms by which TRPM2 regulate autophagy is still poorly understood. In this study, we aimed to identify the changes in autophagic–apoptotic gene expression levels in TRPM2-expressing human prostate adenocarcinomas and to evaluate the effects of TRPM2 inhibition, mediated by small interfering RNA (siRNA), on gene expression levels which have a role in autophagic and apoptotic pathways in PC-3 cell line.

Materials and methods

Cell culture

In the study, PC-3 cell line having high metastatic potential, representative for advanced prostate cancer, expressing high levels of TRPM2, androgen independent, and resistant to many chemotherapy drugs and apoptosis inhibitors was used. RPMI-1640 medium (Cat. No. R0883, Sigma–Aldrich, Germany) containing fetal bovine serum 10% (Cat. No. F6178, Sigma–Aldrich, USA) was used to grow PC-3 cells (ATCC® CRL-1435™). The cells were cultured in incubator (Nuve, Turkey) with 5% CO_2 and 95% air at 37 °C.

siRNA transfection

The PC-3 cells were plated on six-well cell culture plates and transfected with either siRNA specific to TRPM2 (Cat. No. 1027416, Qiagen, USA) or negative control siRNA (Cat. No. 1027280, Qiagen, USA) using HiPerfect® transfection reagent (Cat. No. 301704, Qiagen, Germany) according to the manufacturer's instructions and then incubated for 72 h. Using the TRPM2 human gene test (Cat. No. QT01870407, Qiagen, Germany), quantitative real time-polymerase chain reaction (qPCR) was performed to determine whether silencing was occured. According to the qPCR result, the following calculation method was used to calculate the percentage of siRNA silencing: ΔΔCT mean = ΔCT TRPM2-siRNA–ΔCT negative control; fold change = $2^{-\Delta\Delta CT}$; percentage of silence = 100 × (1–fold change).

3-[4,5-Dimethylthiazol-2-yl]-2,5-diphenyl tetrazolium bromide assay

Colorimetric 3-[4,5-dimethylthiazol-2-yl]-2,5-diphenyl tetrazolium bromide (MTT) (Cat. No. M2128, Sigma–Aldrich, USA) assay was used to determine cell viability. The PC-3 cells were seeded in 96-well plates at a density of 1×10^3 cells per well. Each well was subjected to 100 µl culture medium and 100 µl specific TRPM2 inhibitor 8-bromoadenosine-5′-*O*-diphosphoribose (8-Br-ADPR) (Cat. No. MBS256039, MyBioSource, USA) at different concentrations (1–100 µM) and cultured for 24 or 48 h. MTT (0.5 mg/ml in PBS) was added to the wells and then incubated for 2 h at 37 °C. 100 µl/well of Me_2SO (Cat. No. 320293, Sigma–Aldrich, USA) was added after the removal of MTT solution to dissolve the cells. Absorbance values were measured at 540 nm wavelength via spectrophotometer (BioTek Instruments, USA). Each of the experimental conditions was set to repeat at least three times (Ferreira et al. 2013; Denizot and Lang 1986; Mosmann 1983). Cell count and viability were also measured with an automated cell counter (BioRad TC20, Singapore) by performing trypan blue (0.4%, Cat no: 1450013, Bio-Rad) staining (data not shown).

Acridine orange staining

The PC-3 cells were incubated in six-well plates, filled as 1×10^5 cells per well, for 24 h. The cells were then incubated with dimethyl sulphoxide (DMSO) (Cat. No. D8418, Sigma Aldrich, USA), negative control siRNA, or TRPM2-siRNA administrations for 24 h. At the end of the incubation, the medium was removed and the cells were stained by phosphate-buffered saline (PBS) (Cat. No. P5368, Sigma Aldrich, USA) containing 1 µg/ml acridine orange (AO) (Cat. No. A1301, Invitrogen™, USA) for 15 min at 37 °C

and were examined under a fluorescence microscope (Olympus, Japan) after washing.

Total RNA isolation from cell culture

RNA isolation from the PC-3 cells was conducted with GeneJet RNA Purification kit (Cat. No. K0731, Thermo Scientific, Lithuania) according to the manufacturer's recommended protocol.

Human tissue specimens

Ethical committee approval was obtained from the Ethics Committee for Non-Interventional Studies of Firat University and the research was undertaken with appropriate informed consent of participants. The paraffin blocks of prostate tissues (transurethral resection (TUR) samples) were obtained from the Pathology department of the Faculty of Medicine of Firat University. 180 human prostate tissue samples, taken between 2010 and 2016, were divided into 7 groups according to the gleason score (GS) system of WHO 2016; Control, benign prostate hyperplasia (BPH), grade group 1 (GS ≤ 6), grade group 2 (GS = 7 (3 + 4)), grade group 3 (GS = 7 (4 + 3)), grade group 4 (GS = 8) and grade group 5 (GS = 9–10).

Total RNA isolation from paraffin-embedded tissue samples

Total RNA from paraffin-embedded prostate tissues was extracted using a modification of the methods described by Sharma et al. (2012) and Ma (2012). Briefly, 20 µm thickness five sections were taken into the sterile tubes and incubated for an hour at 65 °C. After the paraffin removal by xylene (Cat. No. 534056, Sigma Aldrich, USA) three times for 5 min, rehydration was carried out through sequential washing 100%, 70%, and 50% ethanol (Cat. No. K32494886-339, Merck, Germany) diluted in nuclease-free water (Cat. No. 7732-18-5, BioShop, Canada). RNA purified by phenol–chloroform extractions was precipitated by the addition of an equal volume of isopropanol (Cat. No. I9516, Sigma, USA) at − 20 °C overnight. The RNA pellet was, respectively, washed with 75% ethanol, dried and resuspended in 10–30 µl of nuclease-free water.

Complementer DNA synthesis

The PCR for complementer DNA (cDNA) synthesis was performed by using a High-Capacity cDNA Reverse Transcription Kit (Cat. No. 4368814. Applied Biosystems, USA) and thermal cycler (Veriti, Applied Biosystems, Singapore) at 25 °C for 10 min, 37 °C for 120 min and 85 °C for 5 min, according to the manufacturer's instructions.

Quantitative polymerase chain reaction analysis

mRNA levels of TRPM2, autophagic and apoptotic genes were analyzed by quantitative polymerase chain reaction (qPCR) in prostate specimens obtained from both paraffin blocks and cell cultures. SYBR-green-based TRPM2 primer (Cat. No. 1027416, Qiagen, USA), autophagy primers (Cat. No. HATPL-I, Human Autophagy Primer Library, RealTimePrimers.com) and apoptosis primers (Cat. No. HPA-I, Human Apoptosis Primer Library, RealTimePrimers.com) were used for the gene expression analysis at mRNA level. In Table 1, the genes, assessed using qPCR analysis in PC-3 cell line or paraffin-embedded prostate tissues, and their properties were given. The mixture required for evaluation of TRPM2 and autophagic–apoptotic gene expressions was prepared with iTaq universal SYBR green supermix (Cat. No. 172–5121, Bio-Rad, USA). mRNA expression levels of the genes were determined by qPCR system (7500 Real Time-PCR, Applied Biosystems, Singapore). In the study, glyceraldehyde 3-phosphate dehydrogenase (GAPDH) (Cat. No. QT00079247, Qiagen, USA) was used as a reference gene. At the end of qPCR analysis, $2^{-\Delta\Delta Ct}$ method was used to calculate the differences in gene expression.

Immunohistochemistry

Immunohistochemical staining was performed in 5 µm sections taken from paraffinized prostate tissue blocks. TRPM2 primary antibody (rabbit polyclonal, Cat. No. PA2231, Boster Immunoleader, Pleasanton, CA) and a biotinylated goat anti-polyvalent secondary antibody [TP–060-BN, Biotinylated Goat Anti-Polyvalent (anti-mouse/rabbit IgG), Thermo Scientific] were diluted at 1:200 with PBS. The incubation times and temperatures for the primary and secondary antibodies were set to 60 min at 37 °C and 30 min at 37 °C, respectively. Streptavidin peroxidase (TS-060-HR, Streptavidin Peroxidase, Thermo Scientific) and 3-amino-9-ethylcarbazol (AEC) solution (TA-060-HA, AEC Substrate System, Thermo Scientific) were used for visualization. Preparations were evaluated and photographed by Olympus BX 50 microscope. The immunohistochemical histoscore was calculated on the basis of immunoreactivity prevalence (0.1: < 25%, 0.4: 26–50%, 0.6: 51–75%, 0.9: 76–100%) and severity (0: no, + 0.5: very little, + 1: little, + 2: medium, + 3: severe) (Histoscore = prevalence × severity).

Statistics

All descriptive and inferential statistical analyses were performed with IBM Statistical Package for the Social Sciences (SPSS) version 22.0 software (Chicago, IL, USA). Depending on data distribution, the Mann–Whitney *U* test or one way ANOVA was conducted for group comparisons.

Table 1 Genes analyzed with qPCR in PC-3 cell line and paraffin-embedded prostate tissue samples

Gene name	Gene symbol	Chromosomal localization	Related pathways
Unc-51-like kinase 1	ULK1	12q24.33	Autophagy induction/cellular senescence/AMPK signaling pathway
Unc-51-like kinase 2	ULK2	17p11.2	Autophagy induction/p53 pathway (RnD)/longevity regulating pathway
RB1-inducible coiled-coil 1	RB1CC1	8q11.23	Autophagy induction
Autophagy-related 2	ATG2A	11q13.1	Autophagy induction
Phosphoinositide-3-kinase, class 3	PIK3C3	18q12.3	Autophagy vesicle nucleation/glucose/energy metabolism and signaling
Phosphoinositide-3-kinase, regulatory subunit 4	PIK3R4	3q22.1	Autophagy vesicle nucleation/CTLA4 signaling / p70S6K signaling
Autophagy/beclin-1 regulator 1	AMBRA1	11p11.2	Autophagy vesicle nucleation/PtdIns3KC3 activation/cell proliferation
SH3-domain GRB2-like endophilin B1	SH3GLB1	1p22.3	Autophagy vesicle nucleation/ER-to-Golgi
UV radiation resistance associated gene	UVRAG	11q13.5	Autophagy vesicle nucleation/vesicle maturation/tumor suppression
Beclin 1	BECN1	17q21.31	Autophagy vesicle nucleation/tumor suppression
Beclin 2	BECN1L1	1q43	Autophagy vesicle nucleation/G-protein coupled receptors turnover
Beclin 1-associated autophagy-related key regulator	BARKOR	14q22.3	Autophagy vesicle nucleation
Autophagy-related 12	ATG12	5q22.3	Autophagy vesicle elongation/induction of immune system
Autophagy-related 5	ATG5	6q21	Autophagy vesicle elongation/induction of IFN-alpha/beta pathways
Autophagy-related 10	ATG10	5q14.1	Autophagy vesicle elongation/senescence
Gamma-aminobutyric acid receptor-associated protein	GABARAP	17p13.1	Autophagy vesicle elongation/vesicle-mediated transport
Autophagy-related 7	ATG7	3p25.3	Autophagy vesicle elongation/innate immune system
Autophagy-related 3	ATG3	3q13.2	Autophagy vesicle elongation/senescence
Autophagy-related 4	ATG4A	Xq22.3	Autophagy vesicle elongation/cellular senescence
Autophagy-related 16-like 1	ATG16L1	2q37.1	Autophagy vesicle elongation/cellular senescence
Microtubule-associated protein 1 light chain 3 alpha	MAP1LC3A	20q11.22	Autophagy vesicle elongation/Pink/Parkin-mediated mitophagy
Microtubule-associated protein 1 light chain 3 beta	MAP1LC3B	16q24.2	Autophagy vesicle elongation/Pink/Parkin-mediated mitophagy
Lysosomal-associated membrane protein 1	LAMP1	13q34	Fusion and degradation stage in autophagy
Lysosomal-associated membrane protein 2	LAMP2	Xq24	Fusion and degradation stage in autophagy
Lysosomal-associated membrane protein 3	LAMP3	3q27.1	Fusion and degradation stage in autophagy
Tumor protein P53	TP53	17p13.1	Glioma and IL-2 pathway
Tumor protein P73	TP73	1p36.32	Gene expression and influenza A
BCL2-associated X protein	BAX	19q13.33	HTLV-I infection and p53 pathway
B-cell CLL/lymphoma 2	BCL-2	18q21.33	Inhibition of beclin 1-dependent autophagy
Transient receptor potential cation channel subfamily M member 2	TRPM2	21q22.3	Ion channel transport and CREB pathway

Pearson correlation coefficient was determined to study relations between variables. The qPCR data were analyzed using the $\Delta\Delta C_t$ module at the QiagenGeneGlobe Data Analysis Center portal: http://www.qiagen.com/us/shop/genesand- pathways/data-analysis-center-overview-page/. The qPCR module transforms threshold cycle (C_t) values to calculate results for gene expression. The efficiency of all the primers used in the study was shown to be over 90%. $p < 0.05$ was considered as significant. Data are expressed as the median and range.

Results

Assessment of cell viability and siRNA transfection efficiency

PC-3 cells were exposed to 8-Br-ADPR, a specific TRPM2 inhibitor, for 24 or 48 h, respectively, and cell viability was measured using MTT assay. Results demonstrated that cytotoxicity in PC-3 cells was induced by 8-Br-ADPR in a time-dependent manner, with all doses of 8-Br-ADPR resulting in a significant decrease in cell viability compared with the untreated control group at 48 h ($p < 0.000$) (Fig. 1a). After the TRPM2-siRNA transfection, TRPM2 mRNA expression level was detected by qPCR. TRPM2 mRNA expression level in TRPM2-siRNA group demonstrated significant decrease compared to the control group ($p = 0.007$). Percentage of TRPM2-siRNA silencing was calculated as 87.5% using gene-silencing calculation method (Fig. 1b).

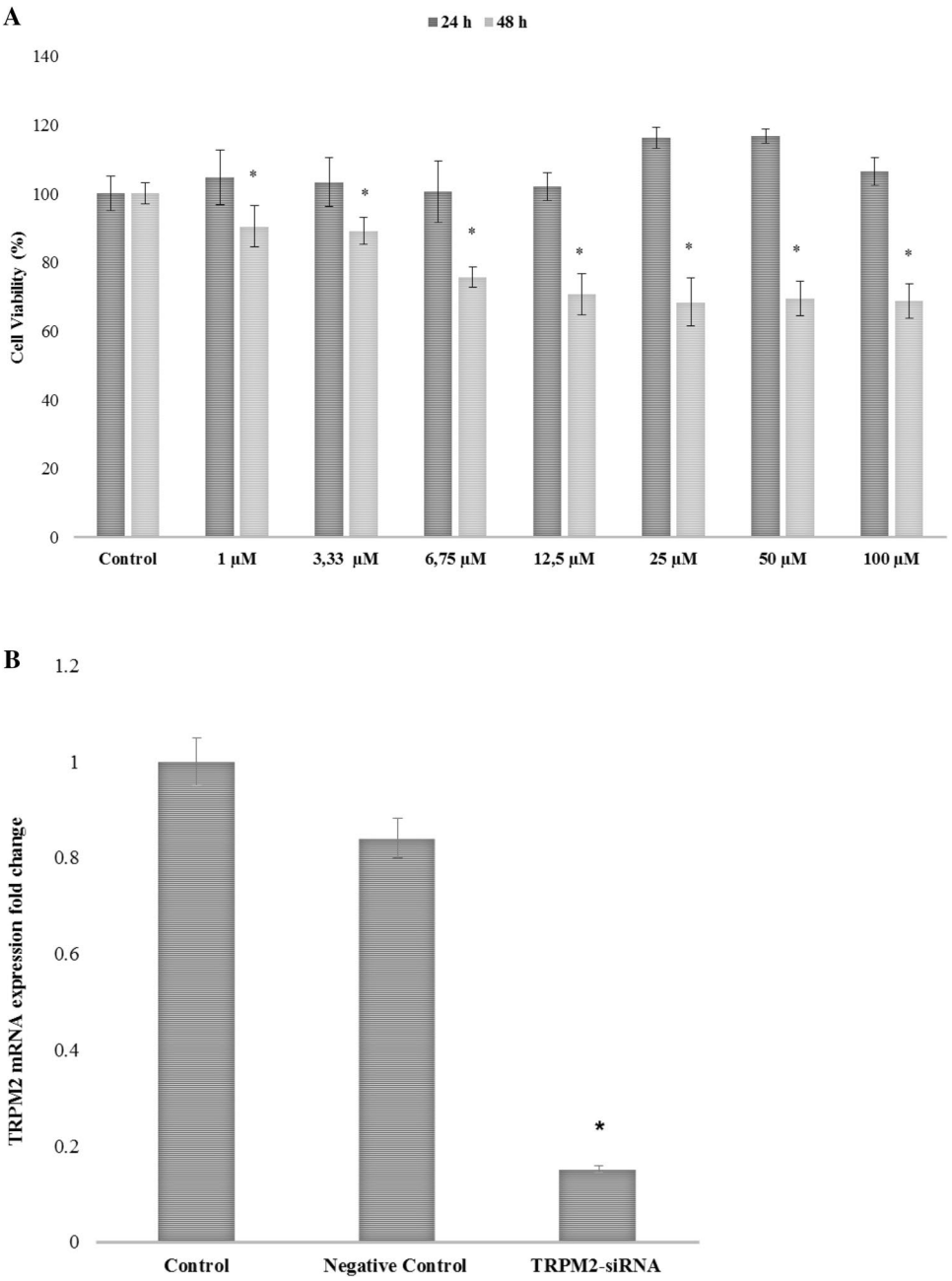

Fig. 1 Cell viability analysis and TRPM2 mRNA expression fold change in PC-3 cells. **a** Bar graph presentation of cell viability. Viability of PC-3 cells was assayed 24 and 48 h after treatment with 1, 3.33, 6.75, 12.5, 25, 50 or 100 µM 8-Br-ADPR. Optical density values of treatment groups were expressed as percentage of viability compared to the DMSO control. Each bar represents the mean value with standard deviation (mean ± SD) from three independent experiments. Data with asterisk significantly differ from DMSO control (Student's *t* test, $*p < 0.05$). **b** Bar graph presentation of TRPM2 mRNA expression levels in control, negative control and TRPM2-siRNA groups. Each bar represents the mean ± SD of three separate experiments performed in 3–9 wells. $*p < 0.05$

Autophagic flux is increased by TRPM2-siRNA transfection in PC-3 Cells

Autophagy induction was determined using AO dye, which is widely preferred in autophagy studies. At the natural pH (pH = 7) AO, a hydrophobic green fluorescent molecule, protonates in acidic vesicle organelles (AVOs) and forms bright red fluorescent-emitting clusters. As shown in Fig. 2, the control and negative control siRNAs showed mostly green fluorescence and very little red fluorescence. This status indicates that there was a small amount of AVOs. However, in TRPM2-siRNA-treated cells, there was an increase in the amount of red fluorescent-emitting clusters compared to control cells ($p < 0.05$) (Fig. 2). This result revealed that TRPM2-siRNA treatment was able to induce autophagy in PC-3 cells.

TRPM2-siRNA transfection in PC-3 Cells increases mRNA expression levels of autophagic and apoptotic genes

The data demonstrate significantly increased mRNA expression levels of Unc-51 Like Kinase 1 (ULK1), Unc-51 Like Kinase 2 (ULK2), Autophagy/beclin-1 regulator 1 (AMBRA1), Beclin 1 (BECN1), Autophagy-related 5 (ATG5), Autophagy-related 16-like 1 (ATG16L1),

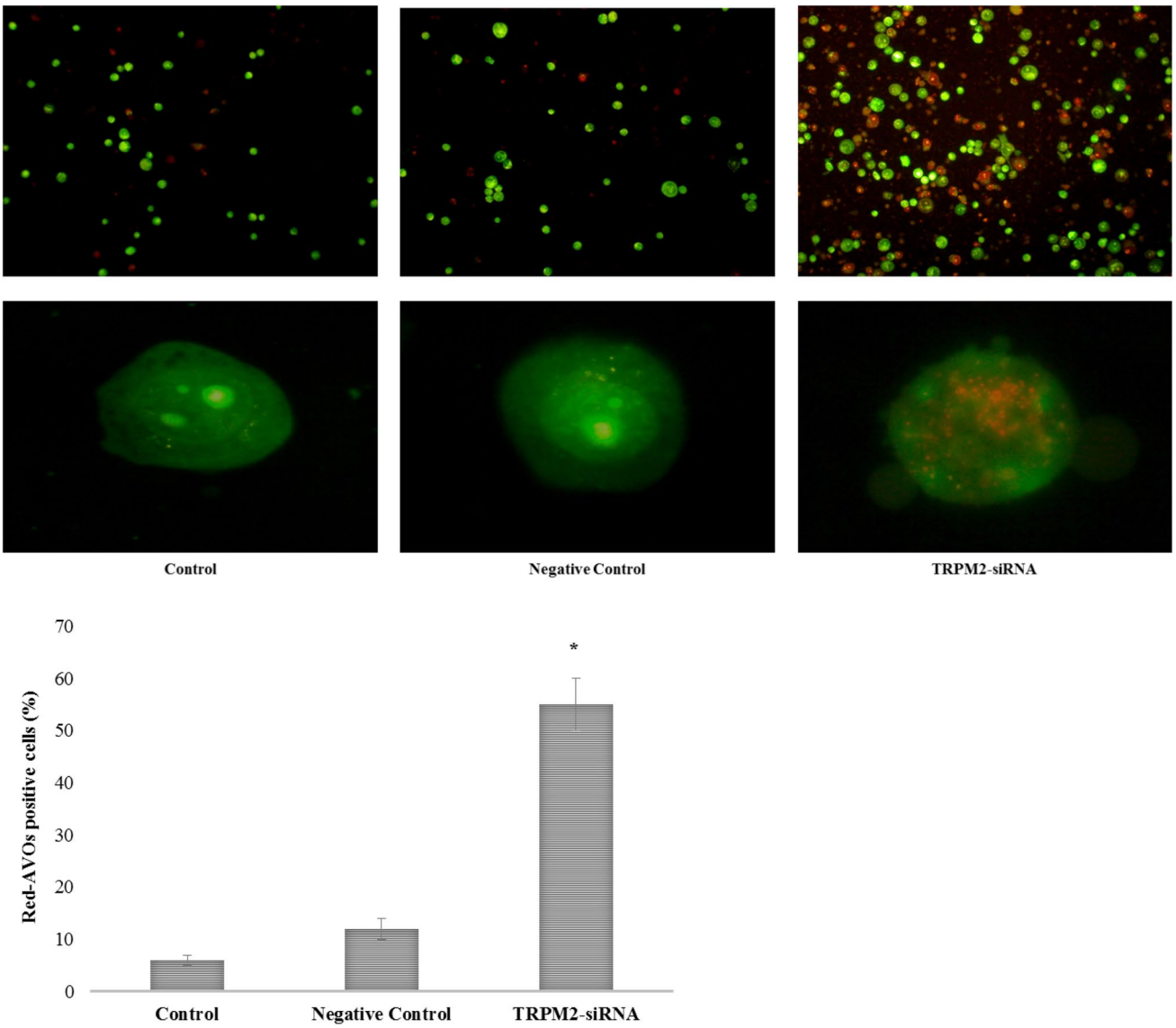

Fig. 2 Acridine orange staining for autophagy study by fluorescence microscopy. AO staining led to an increase in red fluorescent AVOs within the PC3 cells transfected with TRPM2-siRNA. 20 photos were taken at the same magnification (×100 and ×400) and the percentage of cells containing AVO's emitted red fluorescent was calculated for each group. Results are presented in the lower histogram. *$p < 0.05$ (Lin et al. 2017)

Table 2 Comparing to control group fold change (F.C.) and *p* value of mRNA expression levels in human PC-3 cells

Symbol	Negative control		TRPM2-siRNA	
	F. C.	*p* value	F. C.	*p* value
ULK1	0.98	0.943	2.08	0.045
ULK2	3.58	0.016	5.74	0.008
RB1CC1	0.76	0.325	1.27	0.380
PIK3C3	0.64	0.152	0.93	0.786
PIK3R4	0.82	0.454	0.91	0.714
AMBRA1	1.53	0.162	2.48	0.027
SH3GLB1	1.06	0.827	1.88	0.072
UVRAG	0.68	0.207	1.06	0.832
BECN1	2.25	0.039	3.55	0.016
BECN1L1	0.72	0.252	1.04	0.876
ATG12	1.84	0.061	1.65	0.090
ATG5	1.29	0.354	1.98	0.048
ATG16L1	2.41	0.033	3.73	0.015
MAP1LC3A	0.56	0.087	0.69	0.207
MAP1LC3B	0.87	0.583	1.22	0.454
LAMP1	1.65	0.115	2.56	0.025
LAMP2	0.64	0.151	0.82	0.460
LAMP3	0.51	0.059	0.74	0.286
TP53	1.44	0.220	1.57	0.145
TP73	0.93	0.794	1.61	0.130
BAX	1.75	0.096	2.47	0.029
BCL-2	1.28	0.360	0.92	0.753
TRPM2	0.84	0.520	0.15	0.007

Lysosomal-Associated Membrane Protein 1 (LAMP1) and BCL2-Associated X Protein (BAX) in the TRPM2-siRNA group compared with control ($p < 0.05$). On the other hand, there was no statistically significant difference between TRPM2-siRNA and control group in terms of RB1-inducible coiled-coil 1 (RB1CC1), phosphoinositide-3-kinase, class 3 (PIK3C3), phosphoinositide-3-kinase, regulatory subunit 4 (PIK3R4), SH3-domain GRB2-like endophilin B1 (SH3GLB1), UV radiation resistance-associated gene (UVRAG), beclin 2 (BECN1L1), autophagy-related 12 (ATG12), microtubule-associated protein 1 light chain 3 alpha (MAPLC3A), microtubule-associated protein 1 light chain 3 beta (MAPLC3B), tumor protein P53 (TP53), tumor protein P73 (TP73) and B-cell CLL/lymphoma 2 (BCL-2) mRNA expression levels ($p < 0.05$). Furthermore, no significant reduction at the level of mRNA expression of any autophagic gene was observed. mRNA fold changes and *p* values of autophagic–apoptotic genes assessed in PC-3 cells are given in Table 2 and Fig. 3.

Autophagic–apoptotic gene expression levels altered in human prostate adenocarcinoma samples

ULK2, AMBRA1, BECN1, beclin 1-associated autophagy-related key regulator (BARKOR), autophagy-related 10 (ATG10), lysosomal-associated membrane protein 2 (LAMP2) and BAX mRNA expression levels were increased in all groups compared with the control group ($p < 0.05$). It was found that the ATG5 mRNA expression level showed decrease in the BPH, grade group 1, grade group 2, and

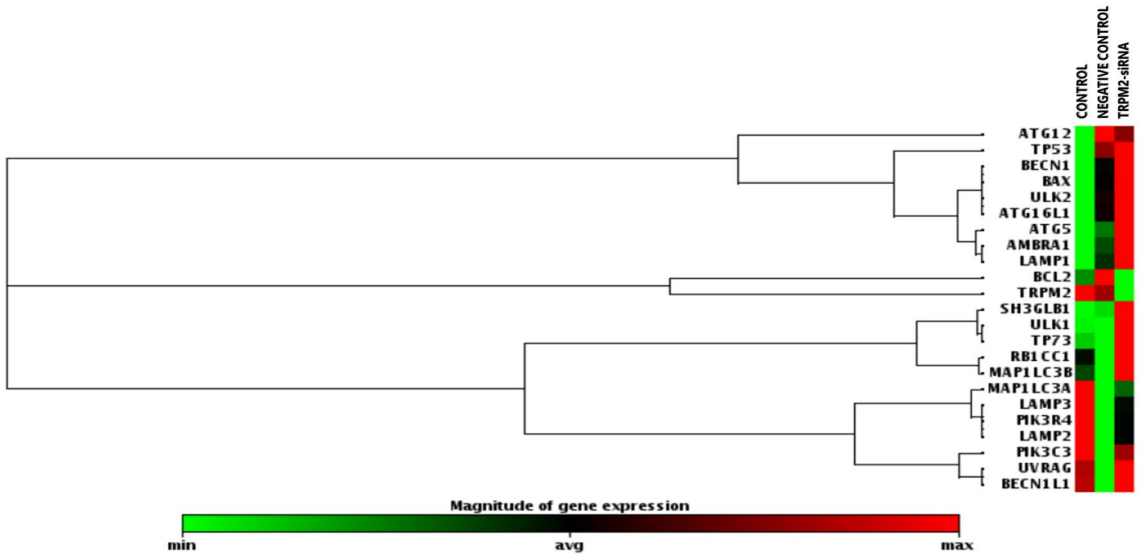

Fig. 3 Heat map graph of gene expression data, clustergram analysis in human PC-3 cells. This analysis was performed using RNAs obtained from PC-3 cells. The mRNA expression obtained using qPCR for the targets selected from the genes in Table 1 is shown as a graph of the profile of the heat map. Genes clustered according to their expression patterns. The red color on the heat map indicates genes that are highly expressed compared to control; green color, genes that are expressed at low level; whereas black color represents genes that are equal to the control

grade group 4 groups compared with the control group ($p < 0.05$). Gamma-aminobutyric acid receptor-associated protein (GABARAP) expression decreased in grade group 1 and grade group 2 groups compared to control group ($p < 0.05$). Autophagy-related 7 (ATG7) expression was found to be increased in all groups except the grade group 5 compared to the control group ($p < 0.05$). The expression of autophagy-related 3 (ATG3) was increased in the grade group 1 and grade group 2 groups compared to the control group ($p < 0.05$). The expression of autophagy-related 4A (ATG4A) showed a decrease only in the grade group 5 ($p < 0.05$). The expression of ATG16L1 was increased in BPH, grade group 1 and grade group 5 groups ($p < 0.05$). TP73 expression was reduced in all groups except grade group 5 compared with the control group ($p < 0.05$). There was no statistically significant change for all the genes except for the differences mentioned above. mRNA fold changes and p values of autophagic–apoptotic genes assessed in human prostate tissue samples are given in Table 3 and Fig. 4. Also, it was found that there was a positive correlation between grade level and ULK2, AMBRA1, BECN1, ATG12, ATG10 mRNA levels and a negative correlation between grade level and RBCC1, ATG4A, LAMP1, TP73, BCL2 mRNA levels.

High grade level in PCa is associated with increased TRPM2 expression

TRPM2 mRNA levels were increased in groups of grade group 2, grade group 3, grade group 4 and grade group 5 compared to control ($p < 0.05$) but it did not change significantly in the other groups. In addition, a significant correlation was found between the grade level increase and the increase in TRPM2 mRNA levels ($r = 0.964$ and $p = 0.000$) (Table 3). TRPM2 protein levels were studied individually for each prostate specimen using immunohistochemical staining (Table 4). Results of qPCR and immunoreactivity were consistent. TRPM2 immunoreactivity was observed in the cytoplasm of gland cells (black arrow) in human prostate tissues (healthy control, BPH and grade group 1–5) using light microscopy (Fig. 5). However, TRPM2 immunoreactivity was not observed in the nucleus or cytoplasm of basal or stromal cells of all samples. TRPM2 was expressed differentially in intensity in the primary prostatic adenocarcinoma of grade levels 1–5. Similar to the luminal cells of benign prostatic glands, TRPM2 was weakly, moderately or strongly expressed in all the tumor glands of grade group 1–5. Among the 40 cases of PCa grade level 1; 30 (75%) showed moderate (+2), 5 (12.5%) showed strong (+3) and 5 (12.5%) showed weak or negative TRPM2 reactivity. In 100 cases of PCa grade level 2–5; 80 (80%) showed strong (+3), 11 (11%) showed moderate (+2) and 9 (9%) showed weak TRPM2 reactivity (Table 5).

Discussion

Treatment options in PCa, especially at the metastatic level, are quite limited and this leads to an increase in mortality. The aim of the study was to determine the molecular mechanisms involved in metastatic PCa. TRPM2 is expressed selectively in a variety of prostate cell lines (normal or cancerous), but it is excessively expressed in PCa compared with normal prostate epithelium or BPH cells (Sikka et al. 2005; Zeng et al. 2010). Thus, it is considered that TRPM2 ion channel can plays a key role in PCa initiation or progression even though its molecular mechanism is not known. Carried out starting from this idea, the main findings we have obtained in the study are as follows. TRPM2 expression significantly increased in parallel with the higher grade levels in human PCa tissue specimens. Furthermore, the expressions of most autophagic genes expressing more mRNAs with the increase of grade level, decreased in the samples with the highest grade levels. Silencing of TRPM2 by siRNA transfection caused significantly increase of autophagic and apoptotic gene expressions at mRNA level. Also inhibition of TRPM2 by 8-Br-ADPR led to significant reduction in cell viability of PC-3 cells. This is the first study to identify TRPM2-siRNA transfection-enhanced specific autophagic gene expression in the PC-3 cell line, 8-Br-ADPR-reduced cell viability in PC-3 cell lines and TRPM2 immunoreactivity in PCa tissues with different grade levels.

Role of TRPM2 channel in Ca^{2+} flow was reported to be critical in hydrogen peroxide (H_2O_2)-induced cell death and autophagy (Chen et al. 2008; Lange et al. 2009; Wang et al. 2016). It has been reported that H_2O_2 induces apoptosis in PC-3 cells but inhibits autophagy. Also when TRPM2 is inhibited in PC-3 cell lines, autophagy is induced for cell survival (Wang et al. 2016). We examined the effects of TRPM2 siRNA on the expression of critical autophagy and apoptosis pathway component genes (ULK1/2, AMBRA1, ATG5, BAX, etc). In this study, we demonstrated that TRPM2 silencing in PC-3 cell lines enhances both autophagic and apoptotic gene expressions similar to Wang et al.'s. Autophagic gene expressions were not analyzed in Wang et al's study. In this respect, this is the first study to show that autophagic gene expressions increase with TRPM2 silencing. TRPM2 plays a role in autophagic mechanisms as well as apoptotic mechanisms in PCa cells. In particular, it was observed that ULK1 and ULK2 involved in the induction phase, AMBRA1 and BECN1 involved in the nucleation phase, ATG5 and ATG16L1 involved in the elongation phase, and LAMP1 mRNA expressions in the fusion phase were significantly increased by TRPM2-siRNA transfection. It

Table 3 Comparing to control group fold change (F.C.) and *p* value of mRNA expression levels in human prostate tissue specimens

Symbol	BPH		Grade group 1		Grade group 2		Grade group 3		Grade group 4		Grade group 5		Pearson correlation	
	F.C.	*p* value	F.C.	*p* value	F.C.	*p* value	F.C.	*p* value	F.C.	*p* value	F.C.	*p* value	*r* value	*p* value
ULK1	1.6358	0.128107	1.0792	0.781579	1.4743	0.187575	1.7532	0.097057	1.2226	0.462068	0.8011	0.413793	− 0.165	0.476
ULK2	2.1886	0.046974	5.0982	0.0091	6.2477	0.008135	3.1383	0.020304	6.5432	0.00678	2.9079	0.020739	0.455	0.038
RB1CC1	0.7371	0.282563	0.727	0.254983	0.8409	0.445853	0.6643	0.174989	0.8293	0.434498	0.669	0.173413	− 0.564	0.008
ATG2A	1.5052	0.165937	2.3784	0.031627	4.3469	0.012281	4.1411	0.013012	2.7895	0.023078	1.5801	0.130287	0.358	0.111
AMBRA1	3.4105	0.018763	7.7812	0.006558	9.7136	0.006337	9.2535	0.005978	12.7286	0.006181	5.579	0.008359	0.650	0.001
UVRAG	0.79	0.394919	1,1728	0.558298	1.2226	0.459285	1.5476	0.161981	0.7974	0.348756	1.007	0.991335	0.119	0.607
BECN1	3.9177	0.013354	5.7757	0.008111	9.5798	0.006899	7.4127	0.008515	11.3137	0.005484	6.2333	0.007623	0.721	0.000
BECN1L1	0.6071	0.120711	1.2658	0.37799	1.4641	0.199546	0.9931	0.959985	0.5783	0.087995	0.6329	0.135594	− 0.318	0.160
BARKOR	3.0738	0.019805	4.6268	0.010086	3.6301	0.013914	3.6808	0.014607	3.6301	0.015959	2.8481	0.021668	0.391	0.080
ATG12	0.683	0.19406	0.5743	0.087264	0.5783	0.087939	1.021	0.932234	1.5369	0.145815	1.1647	0.546985	0.579	0.006
ATG5	0.2643	0.013737	0.3231	0.019177	0.2698	0.014352	0.5625	0.0886	0.2176	0.010785	0.6029	0.114151	− 0.287	0.208
ATG10	3.8906	0.011672	7.3615	0.006785	8.4561	0.006258	9.736	0.00676	6.8211	0.007136	5.6962	0.008208	0.585	0.005
GABARAP	0.7846	0.377221	0.4383	0.042718	0.4175	0.037655	0.3511	0.025243	0.5704	0.085341	0.7371	0.285365	− 0.426	0.054
ATG7	2.3457	0.032381	2.3295	0.034923	3.1602	0.015186	2.9079	0.021859	2.2658	0.039829	1.6702	0.109411	0.258	0.260
ATG3	1.2924	0.356339	2.0705	0.049687	5.3147	0.009394	1.4845	0.182576	0.9727	0.913859	1.5583	0.146993	0.023	0.922
ATG4A	0.669	0.17693	0.6071	0.113591	0.5987	0.111642	0.6156	0.120405	0.7022	0.221019	0.3869	0.026344	− 0.744	0.000
ATG16L1	2.5669	0.029154	2.1735	0.043397	0.9659	0.89487	1.1892	0.518606	1.0718	0.794056	3.0951	0.018313	0.204	0.376
MAPLC3A	0.669	0.175577	0.7684	0.339742	0.7792	0.361903	1.4641	0.207085	0.6552	0.166506	0.7423	0.290057	− 0.028	0.903
MAPLC3B	0.5359	0.069042	0.9526	0.844441	1.7411	0.089065	1.3195	0.307598	0.712	0.231411	0.6242	0.131738	− 0.074	0.750
LAMP1	0.6926	0.207286	0.7684	0.331559	0.6462	0.148512	0.5176	0.058441	0.5105	0.056701	0.6113	0.116937	− 0.812	0.000
LAMP2	11.8762	0.006316	5.3889	0.008557	6.498	0.008575	2.8284	0.021497	3.7064	0.015263	2.6574	0.024682	− 0.299	0.188
LAMP3	1.2058	0.494736	1.3947	0.248241	0.6156	0.130685	1.7654	0.092706	0.8066	0.436028	1.0644	0.816351	− 0.048	0.838
TP53	0.7371	0.292014	1.2924	0.34856	0.722	0.260716	0.7526	0.299477	1.014	0.956835	0.9013	0.682005	− 0.106	0.649
TP73	0.3978	0.029891	0.3015	0.016964	0.1199	0.006819	0.3099	0.018114	0.3392	0.021258	0.5	0.057356	− 0.445	0.043
BAX	6.774	0.008352	18.1261	0.004769	37.5307	0.00426	13.4543	0.004742	14.0257	0.005533	4.6589	0.009956	0.133	0.566
BCL-2	0.5824	0.10683	1.0718	0.795653	0.7579	0.335302	0.5548	0.087376	0.8706	0.604794	0.5704	0.095137	− 0.442	0.045
TRPM2	1.2746	0.371987	1.5052	0.171483	2.2974	0.04038	2.639	0.023875	2.4623	0.031889	3.4822	0.014741	0.964	0.000

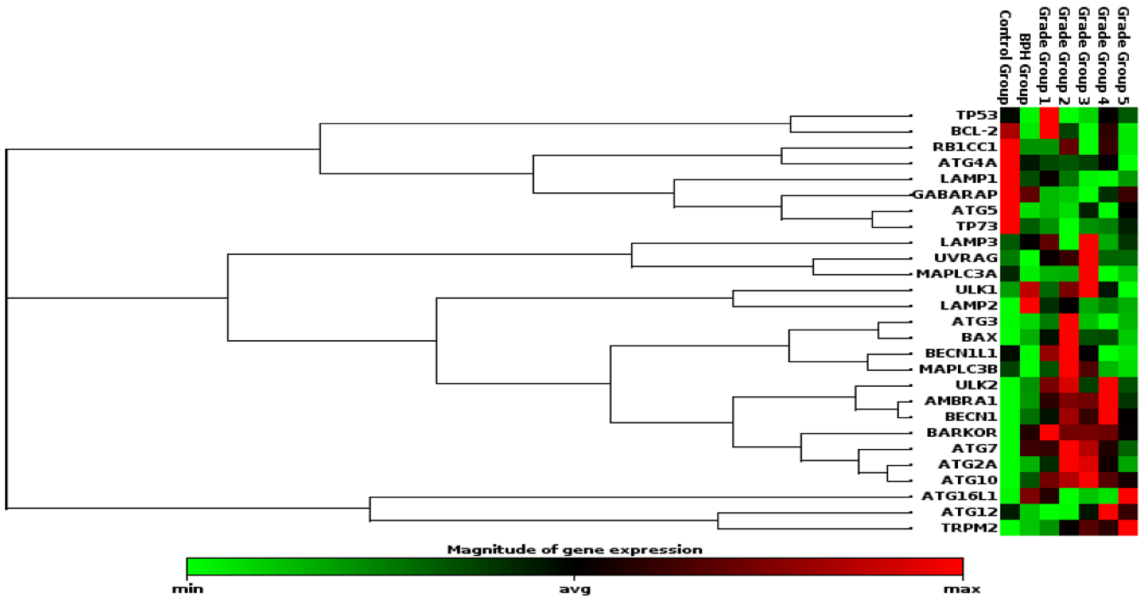

Fig. 4 Heat map graph of gene expression data, clustergram analysis in human tissue specimens. This analysis was performed using RNAs obtained from human paraffin tissue samples. The mRNA expression obtained using qPCR for the targets selected from the genes in Table 1 is shown as a graph of the profile of the heat map. Genes clustered according to their expression patterns. The red color on the heat map indicates genes that are highly expressed compared to control; green color, genes that are expressed at low level; whereas black color represents genes that are equal to the control

has also been determined that TRPM2 silencing increases proapoptotic BAX, one of the genes involved in apoptosis. TRPM2-siRNA transfection in the PC-3 cell line is likely to mediate the rise of cell death and autophagy by increasing the expressions of apoptotic and autophagic genes. In addition, the results from our MTT experiments with 8-Br-ADPR show that 8-Br-ADPR has antitumor activity, especially at 48 h. In this respect, it is thought that TRPM2 silencing or 8-Br-ADPR can be used as therapeutic target in PCa treatment. In future studies, it is important to investigate how 8-Br-ADPR will result in in vivo experiments and what the effects on healthy tissues will be.

Table 4 TRPM2 protein levels of paraffin block prostate tissue specimens for each group

	Undetected	Downregulation	Moderate	Upregulation
Control	–	1 (5%)	16 (80%)	3 (15%)
BPH	1 (5%)	3 (15%)	11 (55%)	5 (25%)
Grade group 1	1 (2.5%)	4 (10%)	30 (75%)	5 (12.5%)
Grade group 2	–	2 (10%)	2 (10%)	16 (80%)
Grade group 3	–	2 (10%)	4 (20%)	14 (70%)
Grade group 4	–	1 (5%)	2 (10%)	17 (85%)
Grade group 5	–	4 (10%)	3 (7.5%)	33 (82.5%)
Total	2	17	68	93

TRPM2 has similar functions in many types of cancer, such as breast and PCa. Its roles in lots of cancer types are most likely survive and proliferation (Blake et al. 2017). Increased TRPM2 expression in PCa has been suggested to be used as prognostic markers (Prevarskaya et al. 2007). The non-coding RNA (ncRNA) transcript of TRPM2, an antisense, (TRPM2-AS) (Orfanelli et al. 2015) may have negative regulatory affects on its sense partner. It was shown that TRPM2-AS is overexpressed both in PCa tissues and tumor cell lines compared to the control. Also it was reported that TRPM2-AS expression is correlated with high GS, metastasis, positive lymph nodes which are poor prognosis indicators. Supressing of TRPM2-AS expression in PCa cells caused apoptosis, so this ncRNA may have a essential role in survival of PCa cells (Lavorgna et al. 2015). Although TRPM2-AS was not assessed in our study, TRPM2 significantly increased when compared to the control from grade level 2 to grade level 5 PCa.

Several recent studies have shown that genes, involved in autophagy, play a crucial role in the etiopathogenesis of cancer (Mowers et al. 2018). The prognostic significance of some autophagic markers in patients undergoing radical prostatectomy was evaluated, some of them potentially related to PCa. (Liu et al. 2015). It has been identified that genetic alterations in PCa that are responsible for autophagy

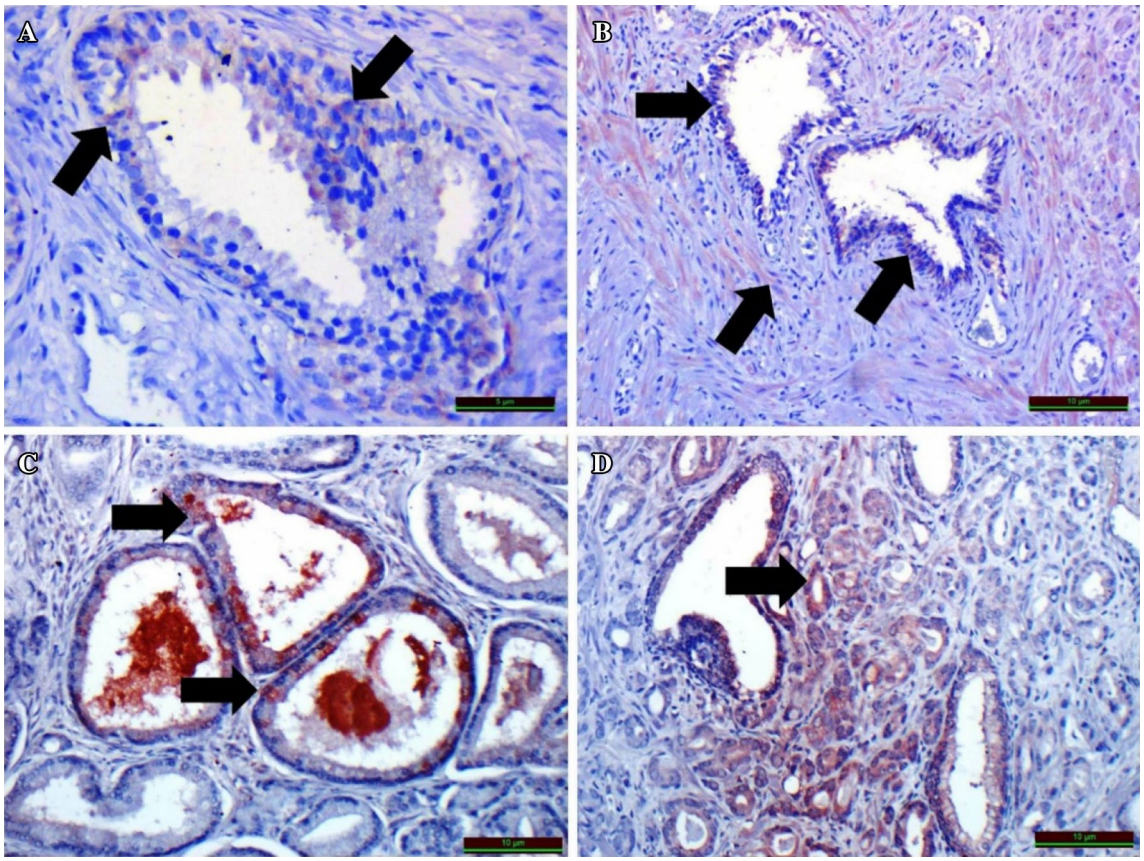

Fig. 5 TRPM2 immunoreactivity in paraffin block prostate tissue specimens. TRPM2 immunoreactivity was clearly observed at cytoplasm of gland cells (black arrow) in the control prostate tissues (**a**), the cytoplasm of the benign glandular cells and surrounding muscle tissue cells (black arrow) in BPH (**b**), the cytoplasm of malignant gland cells (black arrow) in grade group 1 (**c**) and cytoplasm of malignant gland cells (black arrow) in grade group 3 (**d**)

as allele loss in the gene region, amplification, or gene expression changes (Costa et al. 2016). In discussing the findings of our study, for the purpose of establishing a general picture about the expression changes of genes involved in the autophagic stages in PCa have been discussed separately genes involved in each stage such as induction, elongation, nucleation, fusion, and lysis.

Table 5 TRPM2 immunoreactivity histoscore of paraffin block prostate tissue specimens for each group compared with control

Group	Histoscore ± SE (prevalence × severity)	*p* value
Control	0.44 ± 0.11	–
BPH	0.45 ± 0.13	1
Grade group 1	0.43 ± 0.15	0.995
Grade group 2	1.08 ± 0.12	0.011
Grade group 3	1.02 ± 0.13	0.032
Grade group 4	1.1 ± 0.1	0.007
Grade group 5	1.06 ± 0.13	0.021

From the ULK1, ULK2, RB1CC1 and autophagy relates 2A (ATG2A) genes involved in induction of autophagy, the mRNA levels of ATG2A and ULK2 increased, other gene expression no change in PCa than control. ULK1 and ULK2, transcriptional targets of TP53, are upregulated by TP53 in response to DNA damage. This upregulation is essential for the sustained autophagy induced by DNA damage. Thus, the increase in autophagy contributes to subsequent cell death. In light of this information, ULK1 and ULK2 may have an important role in tumor suppression in mammalian cells and can contribute to the efficacy of chemotherapeutic drugs (Gao et al. 2011). Moreover Zhang et al. (2016), reported that in patients with both high expression of ULK1 and leucine-rich PPR motif-containing protein mitochondrial (LRPPRC) were significantly related with GS, serum prostate specific antigen (PSA) levels and metastasis. They also showed that the increased ULK1 expression was significantly correlated with the incidence of biochemical recurrence (BR). It was determined in another study that ULK1 expression level, serum PSA level, pathologic stage, GS, seminal vesicle invasion, and surgical margin status were

significant predictors of BR (Liu et al. 2015). John Clotaire et al. (2016) reported that ULK2 is upregulated both in PCa cells and in tissues. In the present study, although no change was observed in the TP53 expression, the ULK2 expression significantly changed in the PCa compared to the control and BPH tissues. This finding suggests that an increase in ULK2 may also occur independently from TP53. Tang et al. (2017) reported that silencing of ATG2A caused the formation of immature autophagosomal membranes, which induced apoptosis as a result of non-conical caspase-8 activation in the absence of nutrients via an intracellular death-inducing signaling complex (iDISC). In this respect, ATG2A is shown as a new target mediated to cancer cell death. As we showed in our study, it is possible that the increase in expression levels of the ATG2A and ULK2 genes, which act in the induction phase of autophagy, is a mechanism that protects PCa cells from apoptosis.

From the PIK3C3, PIK3R4, AMBRA1, SH3GLB1, UVRAG, BECN1, BECN1L1, and BARKOR genes involved in nucleation stage of autophagy, AMBRA1, BECN1, and BARKOR increased but others did not alter significantly in PCa compared to the control. Falasca et al. (2015), stated that the increased expression of AMBRA1 in PCAs may be a marker of progression. Zhu et al. (2017) reported in their studies of six autophagic protein analysis that the BECN1 and ULK1 expressions decreased in the PCa groups compared to the control, while the ATG5, ATG7 and MAPLC3B expressions did not change. They also stated that as grade and stage increases in PCa, autophagy decreases.

From the ATG12, ATG5, ATG10, GABARAP, ATG7, ATG3, ATG4A, ATG16L1, MAPLC3A, and MAPLC3B genes involved in elongation stage of autophagy, the increase of ATG16L1, ATG7, ATG3, ATG10 gene mRNA levels and the decrease in GABARAP, ATG4A, ATG5 gene mRNA levels were detected in PCa compared to the control. The silencing of ATG3 and ATG7 in PC-3 and DU145 cell lines were shown to increase cell apoptosis induced by AZT5363, an AKT inhibitor (Lamoureux and Zoubeidi 2013). Increased expression of ATG10 is associated with lymphovascular invasion and lymph node metastasis in colorectal cancers. Sotgia et al. (2013) have shown that ATG16L1 specifically increases cancer cell metastasis in their investigations of target genes for cancer treatment. In this respect, the increase of ATG3, ATG7, ATG10, and ATG16L1 gene expressions in PCa tissues can be regarded as important autophagic mechanisms for maintaining cell survival and these genes have potential to be new targets in PCa treatment. Monoallelic loss of the essential autophagy gene ATG5 genes have been frequently found in PCas (Costa et al. 2016). On the other hand, Li et al. (2015), indicated that the ATG5 mRNA expression level is higher in PCa than in BPH tissues. The upregulated expression of ATG5 might play a role in the tumorigenesis of PCa. In the current study, it was shown that there was a decrease in ATG5 expression at BPH, grade level 1, grade level 2, grade level 4 groups compared to the control so that it is compatible with the majority of the work.

GABARAP, which was identified to be reduced in grade level 1, grade level 2, and grade level 3 PCa tissues in our study, is responsible for selective autophagy and cargo recognition in the elongation phase of autophagy. In addition, GABARAP, which functions in the phagophore closure, is not widely used as an autophagic marker although it is similar to the LC3, which functions in the phagophore elongation and is an autophagic marker (Szalai et al. 2015). In fact, the decreased GABARAP mRNA levels are suitable for scoring systems 2–6, 7, 8–10 in the gleason scoring system. Significant changes were observed in autophagic mechanisms, especially in the transition from 6 to 7 between scores.

Monoallelic loss of the essential autophagy gene BECN1, MAPLC3, ATG5 and zinc finger and BTB domain containing 24 (ZBTB24) genes have been frequently found in PCas. The protein expression of BECN1 and MAPLC3 has been demonstrated to be lower in prostate adenocarcinoma than in BPH (Costa et al. 2016). Nevertheless, a recent study has demonstrated that about 35% of PCa shows an overexpression of key autophagy proteins (MAPLC3 and p62) directly related to a high GS, indicating that autophagy signaling may be important for cell survival in high-grade PCa (Naponelli et al. 2015). Significantly, overexpressed MAPLC3B expression was detected in PCa tissues compared to BPH. However, it was found that positive LC3B immunoreactivity in PCa, as a marker of increased autophagy, was independently associated with a reduced disease-specific mortality (Mortezavi et al. 2017). Although we did not perform allelic deletion analysis in our study, we found that there were no changes in the expressions of BECLIN and MAPLC3 when compared to BPH or control tissues.

From the LAMP1, LAMP2 ve lysosomal-associated membrane protein 3 (LAMP3) genes involved in fusion and degredation stages of autophagy, LAMP1 and LAMP3 mRNA expressions did not alter, the expression of LAMP2 gene significantly increased. Overexpression of LAMP1, a heavily glycosylated lysosomal membrane protein, was observed in PCa tissues. Morell et al. (2016) reported that LAMP2 is overexpressed in LNCaP PCa cells, silencing LAMP2 in LNCaP cell lines also inhibits autophagy. In this respect, the increased LAMP2 mRNA in PCa is one of the most important indicators of increased autophagy.

The number of studies searching autophagic gene transcriptoma in PCa is very small and most of the autophagic genes analyzed in the present study were not evaluated in previous PCa studies. Many studies have been carried out to evaluate autophagic gene expressions depending on grade and stage in PCa specimens. In the majority of these studies, a single or a few autophagic gene analyses have been

conducted, and as a result, it has been stated that in some studies autophagy has decreased and in others autophagy has increased in PCa (Zhu et al. 2017). One of the most important findings in the current study is the increase in the expression of ULK2, AMBRA1, BECN1, BARKOR, ATG10, ATG7, ATG16L1, and LAMP2 except for the decrease in ATG5, ATG4A, and GABARAP genes in comparison with the control in BPH and PCa samples of different grade levels. There is no change in the expression of 12 genes that play a role in autophagy. The fact that MAPLC3, the most important autophagic marker, did not change, and the increase in BECN1 and LAMP2 supports the increase of autophagy in PCa. However, there was no significant correlation between the increase in grade level and the increase in gene expression in the altered genes.

As to the apoptosis-related genes analyses that we performed on paraffinized prostate tissues, it was shown that Bax significantly increased, TP53 and BCL-2 did not change, and TP73 decreased significantly in the cancer groups compared to the control.

Autophagic changes in the PC-3 cell line in which TRPM2 is silenced appear to be common to the increase in ULK2 and BECN1 when compared to the PCa tissues expressing TRPM2. Although this data may seem contradictory at first glance, many ion channels and autophagic genes in PCa should not be overlooked as they work together and participate in the process of cancer formation.

Our study has several limitations. In terms of mRNA expressions of autophagic genes some differences were observed in paraffin PCa tissue samples and PC-3 cells. The expression of the PIK3C3, PIK3R4, and SH3GLB1 genes, only assessed in TRPM2-siRNA tranfected PC-3 cells was not analyzed in paraffin PCa tissue samples. However, PC-3 cell lines were shown to express these genes. The most likely reasons for this include the presence of alternative splice variants of these genes and genetic alterations that occur throughout the passage of cell lines. The survival analysis of patients was not performed in our study because this data are not available for most patients. ATG2A, ATG3, ATG4A, ATG7, ATG10, and GABARAP genes only evaluated in paraffinized PCa tissue samples were not studied at PC-3 cell lines due to sample inadequacy. Since our study focused only on performing autophagic gene transcriptomics analysis on different grade levels, no analysis was performed on PSA, lymph node metastasis, or other clinical parameters with these genes. In the recent years, the MTT assay, which has been accepted as the gold standard of cytotoxicity tests for a long time, has led to negative thoughts about the reliability of cell viability data. Although all cell viability and cell count analyzes were also controlled by an automated cell counting device in our study, the necessity of applying another cell proliferation assay is obvious. qRT-PCR, which yields very valuable data, is the most sensitive gene expression method for detecting mRNA levels. However, many events in the cells occur at the protein level and after the proteins are transcribed from the mRNA can undergo different modifications. For these reasons, the data we have obtained must be verified at the protein level.

Conclusion

The data obtained about the relationship between Ca^{2+}-permeable ion channels and autophagy suggest that this association plays a role in cancer and chemotherapy resistance. As a result of further work in this area, new strategies can be developed that can be used to treat cancer. TRPM2-siRNA transfection clearly increases the expression of genes involved in autophagic pathways in PC-3 cells. This data demonstrates that TRPM2 suppression can block apoptosis from one side and activate autophagic mechanisms from the other. It was also determined that autophagy can function in cancer in ways that both cause survival and death of the cell. Determining that autophagy is associated with TRPM2 which may contribute to the development of cancer therapies that target TRPM2 leading to autophagy inhibition or overexpression leading to autophagic killing of the host.

Acknowledgements We would like to acknowledge the helpful comments on this paper received from our reviewers.

Author contributions All authors contributed from the project design to the last version of the article.

Funding This project was supported by the Firat University Scientific Research Projects Unit (Project No: TF.14.37).

Compliance with ethical standards

Conflict of interest The authors declare no conflicts of interest.

Ethical approval During the conduct of the study, the ethical standards of the national ethics committee were fully complied with and written consent was obtained from each participant.

Informed consent Additional informed consent was obtained from all individual participants for whom identifying information is included in this article.

References

Bao BY, Yeh SD, Lee YF (2005) 1α, 25-dihydroxyvitamin D 3 inhibits prostate cancer cell invasion via modulation of selective proteases. Carcinogenesis 27(1):32–42

Blake SD, Tweed CM, McKamey SG, Koh DW (2017) Transient receptor potential, Melastatin-2 (TRPM2) blockade: perspectives on potential novel clinical utility in cancer. Transl Cancer Res 6(2):S342–S347

Borley N, Feneley MR (2009) Prostate cancer: diagnosis and staging. Asian J Androl 11(1):74
Chen Y, Sawyers CL, Scher HI (2008) Targeting the androgen receptor pathway in prostate cancer. Curr Opin Pharmacol 8(4):440–448
Choi AM, Ryter SW, Levine B (2013) Autophagy in human health and disease. N Engl J Med 368(7):651–662
Costa JR, Prak K, Aldous S, Gewinner CA, Ketteler R (2016) Autophagy gene expression profiling identifies a defective microtubule-associated protein light chain 3A mutant in cancer. Oncotarget 7(27):41203
Denizot F, Lang R (1986) Rapid colorimetric assay for cell growth and survival: modifications to the tetrazolium dye procedure giving improved sensitivity and reliability. J Immunol Methods 89(2):271–277
Falasca L, Torino F, Marconi M, Costantini M, Pompeo V, Sentinelli S, Piacentini M (2015) AMBRA1 and SQSTM1 expression pattern in prostate cancer. Apoptosis 20(12):1577–1586
Ferlay J, Soerjomataram I, Dikshit R, Eser S, Mathers C, Rebelo M, Parkin DM, Forman D, Bray F (2015) Cancer incidence and mortality worldwide: sources, methods and major patterns in GLOBOCAN 2012. Int J Cancer 136(5):E359–E386
Ferreira JG, Diniz PMM, De Paula CAA, Lobo YA, Paredes-Gamero EJ, Paschoalin T, Oliva MLV (2013) The impaired viability of prostate cancer cell lines by the recombinant plant kallikrein inhibitor. J Biol Chem 288(19):13641–13654
Flourakis M, Prevarskaya N (2009) Insights into Ca^{2+} homeostasis of advanced prostate cancer cells. Biochim Biophys Acta 1793(6):1105–1109
Gao W, Shen Z, Shang L, Wang X (2011) Upregulation of human autophagy-initiation kinase ULK1 by tumor suppressor p53 contributes to DNA-damage-induced cell death. Cell Death Differ 18(10):1598–1607. https://doi.org/10.1038/cdd.2011.33
Huang X, Jan LY (2014) Targeting potassium channels in cancer. J Cell Biol 206(2):151–162
John Clotaire DZ, Zhang B, Wei N, Gao R, Zhao F, Wang Y, Lei M, Huang W (2016) MiR-26b inhibits autophagy by targeting ULK2 in prostate cancer cells. Biochem Biophys Res Commun 472(1):194–200. https://doi.org/10.1016/j.bbrc.2016.02.093
Kondratskyi A, Yassine M, Kondratska K, Skryma R, Slomianny C, Prevarskaya N (2013) Calcium-permeable ion channels in control of autophagy and cancer. Front Physiol 4:272
Kondratskyi A, Kondratska K, Skryma R, Klionsky DJ, Prevarskaya N (2018) Ion channels in the regulation of autophagy. Autophagy 14(1):3–21
Lamoureux F, Zoubeidi A (2013) Dual inhibition of autophagy and the AKT pathway in prostate cancer. Autophagy 9(7):1119–1120
Lang F, Stournaras C (2014) Ion channels in cancer: future perspectives and clinical potential. Phil Trans R Soc B 369(1638):20130108
Lange I, Yamamoto S, Partida-Sanchez S, Mori Y, Fleig A, Penner R (2009) TRPM2 functions as a Lysosomal Ca^{2+}-release channel in β Cells. Sci Signal 2(71):ra23. https://doi.org/10.1126/scisignal.2000278
Lavorgna G, Montorsi F, Salonia A (2015) Prognostic marker and target in prostate cancer. Aging (Albany NY) 7(10):746–747
Li X, Li C, Zhu LH (2015) Correlation of autophagy-associated gene Atg5 with tumorigenesis of prostate cancer. Zhonghua Nan Ke Xue 21(1):31–34
Lin YC, Lin JF, Tsai TF, Chen HE, Chou KY, Yang SC, Hwang S (2017) Acridine orange exhibits photodamage in human bladder cancer cells under blue light exposure. Sci Rep 7(1):14103
Liu B, Miyake H, Nishikawa M, Tei H, Fujisawa M (2015) Expression profile of autophagy-related markers in localized prostate cancer: correlation with biochemical recurrence after radical prostatectomy. Urology 85(6):1424–1430
Ma Z (2012) Total RNA extraction from formalin-fixed, paraffin-embedded (FFPE) blocks. Bio-protocol 2(7):e161. https://doi.org/10.21769/BioProtoc.161
Mahmoud AM, Yang W, Bosland MC (2014) Soy isoflavones and prostate cancer: a review of molecular mechanisms. J Steroid Biochem Mol Biol 140:116–132
Morell C, Bort A, Vara-Ciruelos D, Ramos-Torres Á, Altamirano-Dimas M, Díaz-Laviada I, Rodríguez-Henche N (2016) Up-regulated expression of LAMP2 and autophagy activity during neuroendocrine differentiation of prostate cancer LNCaP cells. PloS One 11(9):e0162977
Mortezavi A, Salemi S, Rupp NJ, Rüschoff JH, Hermanns T, Poyet C, Wild P (2017) Negative LC3b immunoreactivity in cancer cells is an independent prognostic predictor of prostate cancer specific death. Oncotarget 8(19):31765
Mosmann T (1983) Rapid colorimetric assay for cellular growth and survival: application to proliferation and cytotoxicity assays. J Immunol Methods 65(1–2):55–63
Mowers EE, Sharifi MN, Macleod KF (2018) Functions of autophagy in the tumor microenvironment and cancer metastasis. FEBS J 285(10):1751–1766
Naponelli V, Modernelli A, Bettuzzi S, Rizzi F (2015) Roles of autophagy induced by natural compounds in prostate cancer. Biomed Res Int 2015:121826. https://doi.org/10.1155/2015/121826
Orfanelli U, Jachetti E, Chiacchiera F, Grioni M, Brambilla P, Briganti A, Bellone M (2015) Antisense transcription at the TRPM2 locus as a novel prognostic marker and therapeutic target in prostate cancer. Oncogene 34(16):2094–2102
Ouyang DY, Xu LH, He XH, Zhang YT, Zeng LH, Cai JY, Ren S (2013) Autophagy is differentially induced in prostate cancer LNCaP, DU145 and PC-3 cells via distinct splicing profiles of ATG5. Autophagy 9(1): 20–32
Palmbos PL, Hussain MH (2016) Targeting PARP in prostate cancer: novelty, pitfalls, and promise. Oncology 30(5):377–377
Prevarskaya N, Flourakis M, Bidaux G, Thebault S, Skryma R (2007) Differential role of TRP channels in prostate cancer. Biochem Soc Trans 35(Pt 1):133–135
Ravikumar B, Sarkar S, Davies JE, Futter M, Garcia-Arencibia M, Green-Thompson ZW (2010) Regulation of mammalian autophagy in physiology and pathophysiology. Physiol Rev 90:1383–1435
Reynolds AR, Kyprianou N (2006) Growth factor signalling in prostatic growth: significance in tumour development and therapeutic targeting. Br J Pharmacol 147:S2
Sharma M, Mishra B, Saikia UN, Bahl A, Ratho RK, Talwar KK (2012) Ribonucleic acid extraction from archival formalin fixed paraffin embedded myocardial tissues for gene expression and pathogen detection. J Clin Lab Anal 26(4):279–285
Sikka SC, Zeng X, Jia D, Abdel-Mageed A, Li M (2005) Selective expression of novel TRPM2 calcium channel in human prostate cancer. Cancer Res 65(9 Supplement):556
Sotgia F, Martinez-Outschoorn UE, Lisanti MP (2013) Cancer metabolism: new validated targets for drug discovery. Oncotarget 4(8):1309
Subramani S, Malhotra V (2013) Non-autophagic roles of autophagy-related proteins. EMBO Rep 14(2):143–151
Szalai P, Hagen LK, Sætre F, Luhr M, Sponheim M, Øverbye A, Engedal N (2015) Autophagic bulk sequestration of cytosolic cargo is independent of LC3, but requires GABARAPs. Exp Cell Res 333(1):21–38
Tang Z, Takahashi Y, Chen C, Liu Y, He H, Tsotakos N, Wang HG (2017) Atg2A/B deficiency switches cytoprotective autophagy to non-canonical caspase-8 activation and apoptosis. Cell Death Differ 24(12):2127

Wang Q, Guo W, Hao B, Shi X, Lu Y, Wong CW, Cheung KH (2016) Mechanistic study of TRPM2-Ca2+-CAMK2-BECN1 signaling in oxidative stress-induced autophagy inhibition. Autophagy 12(8):1340–1354

White E (2015) The role for autophagy in cancer. J Clin Investig 125(1):42

Zeng X, Sikka SC, Huang L, Sun C, Xu C, Jia D, Li M (2010) Novel role for the transient receptor potential channel TRPM2 in prostate cancer cell proliferation. Prostate Cancer Prostatic Dis 13(2):195

Zhang HY, Ma YD, Zhang Y, Cui J, Wang ZM (2016) Elevated levels of autophagy-related marker ULK1 and mitochondrion-associated autophagy inhibitor LRPPRC are associated with biochemical progression and overall survival after androgen deprivation therapy in patients with metastatic prostate cancer. J Clin Pathol 70(5):383–389. https://doi.org/10.1136/jclinpath-2016-203926

Zhu L, Deng X, Chen H, Liu R, Luo J, Peng G (2017) Analysis of the expression of autophagy-related protein in prostate cancer and preliminary investigation of its clinical significance. Biomed Res 28(14):6518–6523